



RESEARCH ARTICLE

Comparative analysis of leaf area index and maize yield estimation assimilating remote sensing and DSSAT crop simulation model

Hemareddy Thimmareddy¹, Pazhanivelan S², Ragunath KP², Sathyamoorthy NK¹, Sivamurugan AP², Vincent S³, Sudarmanian NS², Satheesh S⁴ & Pugazenthi K¹

¹Agro Climate Research Centre, Tamil Nadu Agricultural University, Coimbatore, Tamil Nadu - 641003, India

²Centre for Water and Geospatial Studies, Tamil Nadu Agricultural University, Coimbatore, Tamil Nadu - 641003, India

³Department of Crop Physiology, Tamil Nadu Agricultural University, Coimbatore, Tamil Nadu - 641003, India

⁴Department of Remote Sensing and GIS, Tamil Nadu Agricultural University, Coimbatore, Tamil Nadu - 641003, India

*Email: pazhanivelans@tnau.ac.in



ARTICLE HISTORY

Received: 20 August 2024

Accepted: 08 September 2024

Available online

Version 1.0 : 19 September 2024

Version 2.0 : 01 October 2024



Additional information

Peer review: Publisher thanks Sectional Editor and the other anonymous reviewers for their contribution to the peer review of this work.

Reprints & permissions information is available at https://horizonepublishing.com/journals/index.php/PST/open_access_policy

Publisher's Note: Horizon e-Publishing Group remains neutral with regard to jurisdictional claims in published maps and institutional affiliations.

Indexing: Plant Science Today, published by Horizon e-Publishing Group, is covered by Scopus, Web of Science, BIOSIS Previews, Clarivate Analytics, NAAS, UGC Care, etc See https://horizonepublishing.com/journals/index.php/PST/indexing_abstracting

Copyright: © The Author(s). This is an open-access article distributed under the terms of the Creative Commons Attribution License, which permits unrestricted use, distribution and reproduction in any medium, provided the original author and source are credited (<https://creativecommons.org/licenses/by/4.0/>)

CITE THIS ARTICLE

Thimmareddy H, Pazhanivelan S, Ragunath KP, Sathyamoorthy NK, Sivamurugan AP, Vincent S, Sudarmanian NS, Satheesh S, Pugazenthi K. Comparative Analysis of Leaf Area Index and Maize Yield Estimation Assimilating Remote Sensing and DSSAT Crop Simulation Model. Plant Science Today. 2024; 11(4): 137-148. <https://doi.org/10.14719/pst.4736>

Abstract

Maize is a global staple crop, impacting food security, economic development, and agricultural sustainability. This study investigates the integration of Sentinel-1A Synthetic Aperture Radar (SAR) data with the DSSAT CERES-Maize crop simulation model to estimate Leaf Area Index (LAI) and *rabi* maize yield in Belagavi district, Karnataka. Field data, including LAI, days to anthesis, silking, grain filling and farmers' field practices, were collected for model calibration and validation, supplemented by crop-cutting experiments (CCE) to determine actual yields. The study revealed strong correlations between LAI values obtained from remote sensing (RS) and field observations, with RS-derived LAI showing an average agreement of approximately 96.07% compared to field measurements. The DSSAT model exhibited slightly better performance, averaging 97.09%. Statistical analysis for LAI showed an R^2 value of 0.853 for RS and 0.864 for DSSAT, indicating strong correlations with observed LAI values. For maize yield estimation, the DSSAT model demonstrated higher accuracy with an average yield of 8129 kg/ha, compared to RS-derived yield averages of 7533.9 kg/ha and CCE yield averages of 8096.6 kg/ha. The average concordance between DSSAT and CCE yields was 94.19%, while RS and CCE yields had an average concordance of 92.29%. Statistical analyses revealed coefficients of determination of 0.854 for DSSAT-CCE and 0.867 for RS-CCE comparisons. The study underscores the value of combining RS data with DSSAT for comprehensive and accurate crop yield forecasting, highlighting the potential for improved agricultural assessments and decision-making.

Keywords

Sentinel 1A; Temporal Backscattering; Synthetic Aperture Radar; Remote sensing; DSSAT; Maize yield

Introduction

Agriculture is a crucial contributor to both national and international economies. Globally, it accounts for around 4% of GDP, while in the case of India it is 18.2%. This share can rise to over 25% in many developing countries, which is vital to economic stability (1). Agriculture is also a significant source of employment, engaging approximately 26.5% of the global workforce, with much higher figures in low-income nations, where up

to 60-70% of the population depends on it for their livelihoods (2). As the global population grows, currently surpassing 8.1 billion in 2023, the demand for food is expected to rise significantly, necessitating innovations in agricultural practices to ensure productivity and sustainability (3). Thus, estimation of yield becomes paramount for farm planning and management. Accurate yield predictions help governments and organizations anticipate food shortages or surpluses, manage grain reserves, and stabilize food prices (4). Traditional yield estimation methods, such as Crop Cutting Experiments (CCE), involve physically harvesting a portion of the crop and extrapolating the results to estimate total yield (5). While CCEs are considered accurate, they are resource-intensive and often not feasible for large-scale applications (6).

To monitor crop growth and forecast yields non-invasive and scalable, remote sensing (RS) presents a competitive option for large-scale yield estimates. Crop health and growth phases, directly tied to yield potential, may be evaluated by analyzing RS data, such as vegetation indices and spectral reflectance patterns (7). By adding environmental and management aspects, RS data may be linked with crop simulation models, such as DSSAT, to improve yield forecast accuracy (8).

Among crop simulation models, the Decision Support System for Agro technology Transfer (DSSAT) is the most used worldwide. DSSAT is a worldwide partnership that simulates crop growth, development and yield by integrating meteorological, soil and crop management data (9). By simulating the biological processes that control crop development, the model enables users to evaluate the effects of various management techniques and environmental factors on crop performance. DSSAT is a valuable instrument for yield assessment and agricultural research since it has been widely verified and used in various agro-ecological zones. The model is beneficial for evaluating the possible effects of climate change on agriculture and for creating adaptation strategies since it can simulate crop responses to changing weather conditions, soil types and management approaches (10).

The advantages of both methods are combined by incorporating remote sensing data into crop simulation models. Crop models may be updated and calibrated using real-time, high-resolution data from remote sensing, which makes the models' forecasts more accurate and true to the field (11). This fusion improves yield projections by strengthening their resistance to uncertainties and fluctuations in weather, pests and illnesses. Furthermore, this integrated approach makes early warning systems and prompt intervention tactics easier. For example, abnormalities found by remote sensing can start simulations that forecast possible yield losses, allowing for proactive risk mitigation. This is essential for ensuring food security because it enables more effective resource management and reduces financial losses for farmers (12). The study addresses the need for timely and accurate agricultural information using an integrated approach. This is important because it can help improve yield predictions,

optimize crop management practices and ensure sustainable agricultural development in areas like Belagavi district, the second-largest rabi maize producer in Karnataka, India. It covers an area of 64,714 hectares, with a total production of 2.73 lakh tonnes and a productivity of 4.23 tonnes per hectare (12).

Materials and Methods

Study area

The Belagavi district is situated in the northwest region of Karnataka, India. It is roughly between latitudes 15°23' and 16°58' N and longitudes 74°5' and 75°28' E (Fig. 1). With the Western Ghats to the west and the plains to the east, its geography is varied, which contributes to its changeable climate. A distinct rainy season, which runs from June to September, is followed by a dry season (14). The district is subject to a tropical monsoon climate. Over 2,500 mm of rain falls annually in the western portion of the area, compared to 700-900 mm in the eastern section. This represents a significant variation in yearly rainfall. Agribusiness is supported by the region's average temperature, which varies from 15°C in the winter to about 35°C in the summer (15).

Ground Truth Data collection and CCE

Ground truth is an essential component of crop classification, as it is used to validate the accuracy of classification algorithms and as an input for their development (16). When collecting ground truth data, specifics like the crop name, coverage, condition, growth stage, irrigation status (irrigated or rainfed), expected yield and sowing and harvesting dates are usually included. Ground truth data about land use and cover is gathered (17). Using a stratified sampling technique, this data was collected from specific sample locations throughout the research region, guaranteeing thorough coverage of various kinds. In all, 369 ground truth points (GTP)-crop and non-crop sites-were gathered for this investigation. Classification, validation and accuracy evaluation were then conducted using these points. Crop Cutting Experiments (CCE) were performed at more than 70 locations and 30 were finalized as monitoring sites to validate yield spread across the district.

Satellite data

Utilizing the Sentinel-1A satellite equipped with the C-SAR instrument provides reliable and extensive monitoring capabilities (18). Synthetic Aperture Radar (SAR) offers a notable benefit, as it operates at wavelengths unaffected by cloud cover or lack of illumination, enabling continuous data collection regardless of the time of day (19). Sentinel-1's various imaging modes, with different resolutions and dual polarization, ensure comprehensive coverage and detailed observations (20). Ground Range Detected (GRD) and Single Look Complex (SLC) datasets from Sentinel-1A SAR, featuring VV and VH polarizations in Interferometric Wide (IW) swath mode, were collected at 12-day intervals. These datasets were essential for crop identification and mapping in the study area. Data from August 29, 2022, to

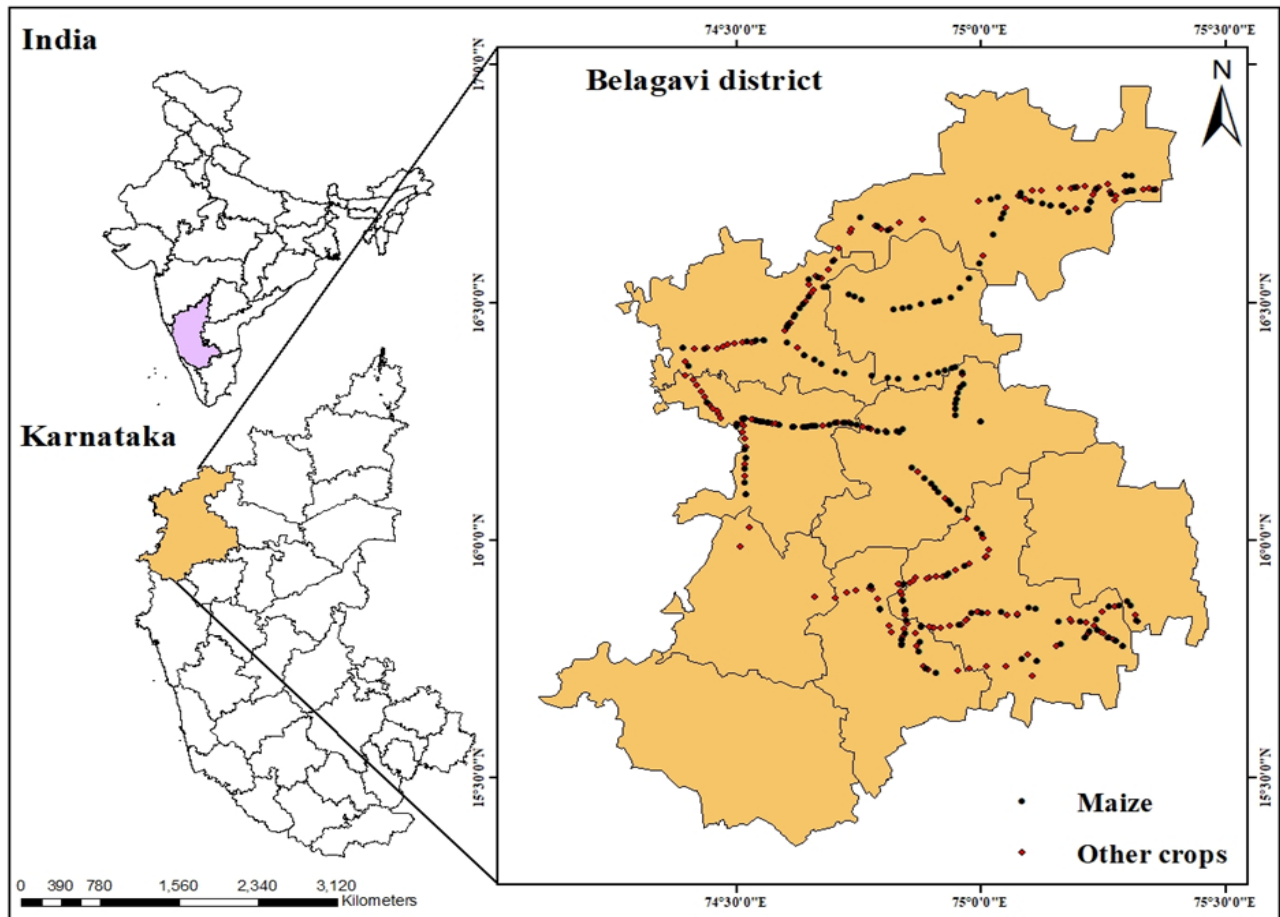


Fig. 1. Study area map with ground truth points

February 25, 2023, were sourced from the Alaska Satellite Facility (<https://asf.alaska.edu/>). This period corresponds with the typical Maize growing season in the study region, ensuring complete coverage of all crop growth stages (Table 1).

Integrating SAR-based remote sensing products and crop simulation model

Crop yield simulation using the DSSAT model

Under the sponsorship of IBSNAT, USA, the Decision Support

System for Agro technology Transfer (DSSAT) was developed through global cooperation (9). The meteorological, crop and soil databases are combined into standard formats by the DSSAT software program for assessment. Next, for every crop in any part of the world, the user can duplicate the outcomes of crop management techniques across several years. For this reason, the current study used the DSSAT crop simulation model. Crop growth and development of Maize were simulated daily by the CERES-Maize model, which was included in the DSSAT v. 4.8 version.

Table 1: Date of satellite pass with mean temporal backscattering (dB) values for the maize monitoring site and crop calendar

S.No	Date of Pass	dB value	Crop Calendar for Rabi Maize			
D1	29.08.2022	-17.50				
D2	10.09.2022	-17.50				
D3	22.09.2022	-17.64				
D4	04.10.2022	-17.61	Sowing Window			
D5	16.10.2022	-17.80				
D6	28.10.2022	-18.42				
D7	09.11.2022	-17.98		Vegetative stage		
D8	21.11.2022	-18.31				
D9	03.12.2022	-17.94			50 % anthesis	
D10	15.12.2022	-17.47				
D11	27.12.2022	-17.32			Grain filling	
D12	08.01.2023	-17.39				
D13	01.02.2023	-17.52				50 % Dough stage
D14	13.02.2023	-17.74				
D15	25.02.2023	-18.31				Maturity/Harvest

Input data for the DSSAT crop simulation model

Weather data

The minimum required weather variables are Maximum and Minimum Temperature ($^{\circ}$ C), Solar Radiation (MJ m^{-2}) and Precipitation at daily time scale. Daily weather data for the 30 monitoring sites of each district for the cropping period of *Rabi* 2022-23 was collected from the NASA Power web portal (<https://power.larc.nasa.gov/>), available in 0.5×0.625 -degree resolution. The daily data was checked for errors and missing values and was corrected. The Weatherman tool was used to create the weather file as an input to the model (Fig. 2).

Soil data

The soil data utilized in this study was collected from the International Research Institute for Climate and Society

(IRICS) at Michigan State University and the International Food Policy Research Institute's (IFPRI) database. These data, available at a scale of 1:10,000 with a 5-minute resolution, offer detailed insights into soil characteristics (<https://doi.org/10.7910/DVN/1PEEYO>).

Crop Management data

The primary maize hybrids in the Belagavi district are 900-M-Gold, DKC-9141, NK-9141 and DKC-9133 (Table 2). Field visits were conducted during the *rabi* season of 2021-22 and 2022 - 23, i.e., the first week of October (vegetative stage), the third week of November (flowering stage) and the first week of January (harvesting stage). Crop management and other operations, viz., land preparation, initial soil conditions, planting geometrics, irrigation and water management, fertilizer management, organic residue application, chemical applications, environment modifications, etc., were gathered by interacting with

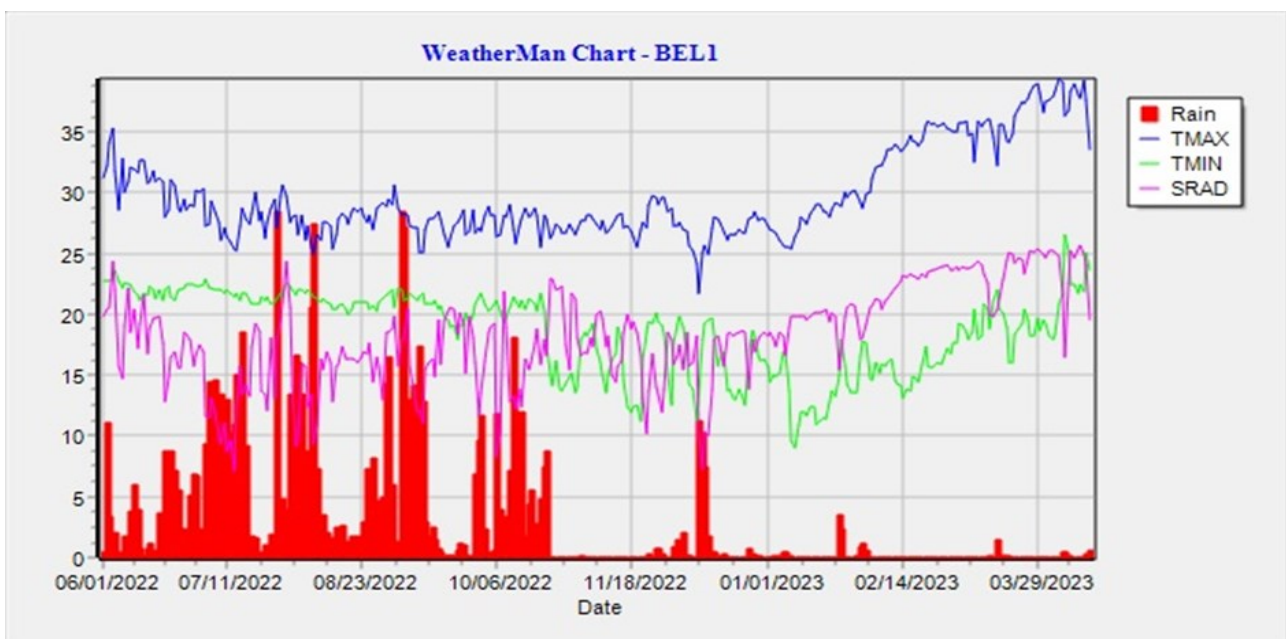


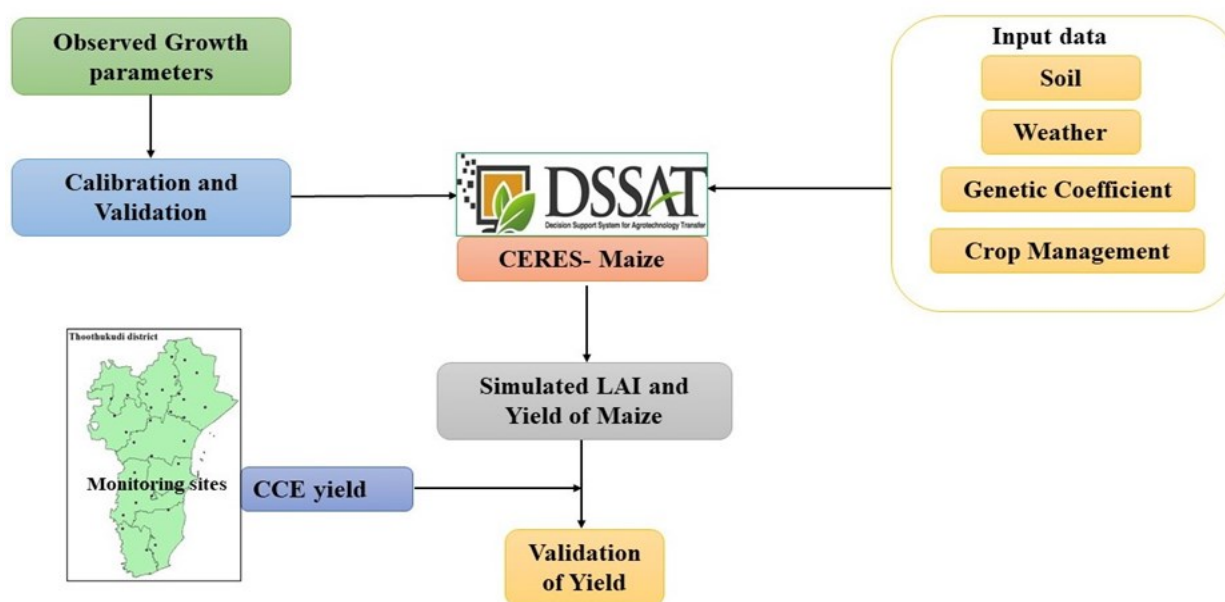
Fig. 2. Created weather file for DSSAT model for one of the monitoring sites of Belagavi district

Table 2: Description of Maize varieties considered for the study

S. No	Particulars	900-M-Gold	NK-6240	DKC-9141	DKC-9133
1.	Duration	110-120 days	110-125 days	115-125 days	110 days
2.	Season	Irrigated: June-Sept (<i>Kharif</i>) Oct- Jan (<i>Rabi</i>) Feb-May (<i>Zaid</i>)	Irrigated: June-Sept (<i>Kharif</i>) Oct- Jan (<i>Rabi</i>) Feb-May (<i>Zaid</i>) Rainfed: June-Sept (<i>Kharif</i>) Oct- Jan (<i>Rabi</i>)	Irrigated: June-Sept (<i>Kharif</i>) Oct- Jan (<i>Rabi</i>) Feb-May (<i>Zaid</i>)	Irrigated: June-Sept (<i>Kharif</i>) Oct- Jan (<i>Rabi</i>) Feb-May (<i>Zaid</i>) Rainfed: June-Sept (<i>Kharif</i>) Oct- Jan (<i>Rabi</i>)
3.	Grain yield	Irrigated: 6500 - 8500 kg/ha ◆ Attractive orange colour kernels with good keeping quality ◆ Good tip-filling, compact ears	Irrigated: 6500 - 7500 kg/ha Rainfed: 5500 - 6500 kg/ha ◆ An orange-yellow dent with bold kernels with excellent tip. ◆ It is a very uniform and appealing plant type.	Irrigated: 6500 - 8500 kg/ha ◆ Good stay green character with high fodder yield, suitable for 26000 plants per acre density. ◆ Robust Big Ears with more rows per cob	Irrigated: 6000 - 7500 kg/ha Rainfed: 5500 - 6000 kg/ha ◆ Bold, attractive grains, good colour, good kernel quality ◆ Stable-yielding hybrid suitable for rainfed conditions
4.	Salient features	◆ Wider adaptability ◆ High-yielding hybrid suitable for assured rainfall and support irrigation geographies.	◆ Widely adapted hybrid with outstanding yield and stability. ◆ Stable yielder across the environments, good responsiveness to high input management.	◆ Relatively better tolerant to stalk rot ◆ It is a high-yielding, input-responsive hybrid suitable for irrigated and assured rainfall areas.	◆ Wider adaptability, tolerance to low moisture stress and response to high inputs, good management and planting density.

Table 3: Genetic co-efficient (GC) of Maize used in DSSAT CERES-Maize model

GC code	Description	Genetic co-efficient			
		NK-6240	DKC-9141	DKC-9133	900-M-GOLD
P1	Thermal time from seedling emergence to the end of the juvenile phase (expressed in degree days above a base temperature of 8°C) during which the plant is not responsive to changes in photoperiod.	169.6	265.0	212.0	262.3
P2	The extent to which development (expressed as days) is delayed for each hour increases in photoperiod above the longest photoperiod at which development proceeds at a maximum rate (considered 12.5 hours).	0.243	0.27	0.270	0.159
P5	Thermal time from silking to physiological maturity (expressed in degree days above a base temperature of 8°C).	934.1	940.0	869.4	930.0
G2	Maximum possible number of kernels per plant.	918.0	920.0	920.0	890.0
G3	Kernel filling rate during the linear grain filling stage and under optimum conditions (mg day ⁻¹).	8.00	8.00	8.00	8.00
PHINT	Phyllochron interval; the interval in thermal time (degree days) between successive leaf tip appearances.	36.76	39.0	38.7	38.90

**Fig. 3.** Schematic representation of methodology of DSSAT CERES-Maize crop simulation model

farmers and the Department of Agriculture officials.

Cultivar file

The cultivar files described the genetic coefficients of the cultivars 900-M-Gold, DKC-9141, NK-9141 and DKC-9133. The genetic coefficients needed for Maize in the DSSAT CERES-Maize model are represented in Table 3.

Model Calibration and Validation

Three input files were compiled to run the DSSAT model using collected datasets. To compute the genetic coefficient for 900-M-Gold, DKC-9141, NK-9141 and DKC-9133 varieties with spatial analysis mode in DSSAT, the model was calibrated using data gathered during the 2021-22 *rabi* Maize crop growing season and was validated with the 2022-23 yield data. Actual yield information from the farmer's fields in the research area was collected as observed yield data. The quality of the simulation results was assessed using various criteria, including the coefficient of determination (R^2), which measures the proportion of variance in the observed data explained by the model. Additionally, root mean square error (RMSE) was used to evaluate the average magnitude of prediction errors,

indicating how closely the simulated values match the observed data. Normalized root mean square error (NRMSE) was also employed to provide a scaled measure of prediction error, facilitating comparisons across different datasets or units. Graphs between the observed and simulated values were created to quickly assess the modelling accuracy using linear regression and the correlation coefficient. The model was then run for the 30 monitoring sites (Fig. 3) and simulated the yields.

Observed LAI from monitoring sites

Five plants were randomly selected during the ground truthing process for each monitoring site to validate the observed LAI and compare it with the crop simulation model and remotely sensed data LAI. Typically, this output was based solely on the phenological and physiological mechanisms that control plant qualities. It was determined by taking one-month interval measurements of the length and width of the fully expanded third leaf starting at 30 DAS and continuing until harvest.

$$LAI = \frac{L \times W \times K \times \text{No. Of Leaves}}{\text{Spacing (cm)}}$$

Where,

L- Length of the leaf (cm), W-Width of the leaf (cm), K- Constant factor (0.70)

For every field, six to ten Leaf area measurements were obtained; the average was then computed to determine the LAI. At the end of the growing season, yield data from each field were collected from the farmer's fields. Finally, from the available data, 30 monitoring sites spread across the research region were selected to supply data to the CERES-Maize module for simulation and validation. Regression analysis was performed by combining the study region's data into a single dataset and comparing the predicted yield with the observed yield.

Retrieving LAI from dB images of SAR data

The dB (backscattering) values of maize fields were acquired from monitoring fields using a point sampling tool in QGIS. A linear regression between the simulated LAI values and the dB values was created using the simulated LAI values from monitoring the maize fields in the research region. Selection queries were made using Map Algebra syntax. Mathematical calculations were done using operators and functions with the QGIS raster calculator tool. Using a raster calculator, point-specific LAI was created in this study by replacing the calculated regression values with dB values in dB photos taken during the crop's flowering stages.

Maize yield estimation assimilating remote sensing techniques with the DSSAT model

The DSSAT simulated yield was integrated with the remote sensing data using LAI values extracted from dB images of

the SAR data. A linear regression equation was created to calculate Maize yield for the research area using the DSSAT simulated yield and spatially simulated LAI values (Fig. 4).

Results

Leaf Area Index Estimation

The analysis of Leaf Area Index (LAI) estimates from Remote Sensing (RS) and the DSSAT model, compared to observed LAI values across 30 samples, shows varying levels of agreement. The RS-derived LAI exhibited percentage agreement with observed LAI values ranging from 91.54 % to 99.79 %, with an average congruence of approximately 96.07 % (Fig. 5). The RS model's performance is quantified by an R^2 value of 0.853 (Fig. 6), indicating a strong correlation with observed LAI. However, the Root Mean Square Error (RMSE) of 0.1396 and Normalized Root Mean Square Error (NRMSE) of 4.09 % suggest some discrepancy between RS predictions and observed values. The spatial LAI estimated has been depicted in Fig. 8.

The DSSAT model, on the other hand, showed slightly higher accuracy, with percentage agreement ranging from 93.55 % to 99.02 % and an average agreement of 97.09 % (Fig. 5). The model's R^2 value of 0.864 (Fig. 6) indicates a robust correlation with observed LAI, marginally outperforming the RS model. The DSSAT model also demonstrated lower RMSE (0.1217) and NRMSE (3.46 %) values, suggesting a closer alignment with the observed data.

Maize Yield Estimation

The comparative analysis of yield data from DSSAT, Remote Sensing (RS), and Crop Cutting Experiment (CCE) sources reveals notable differences in their performance. The DSSAT model showed an average yield of 8129 kg/ha, while RS

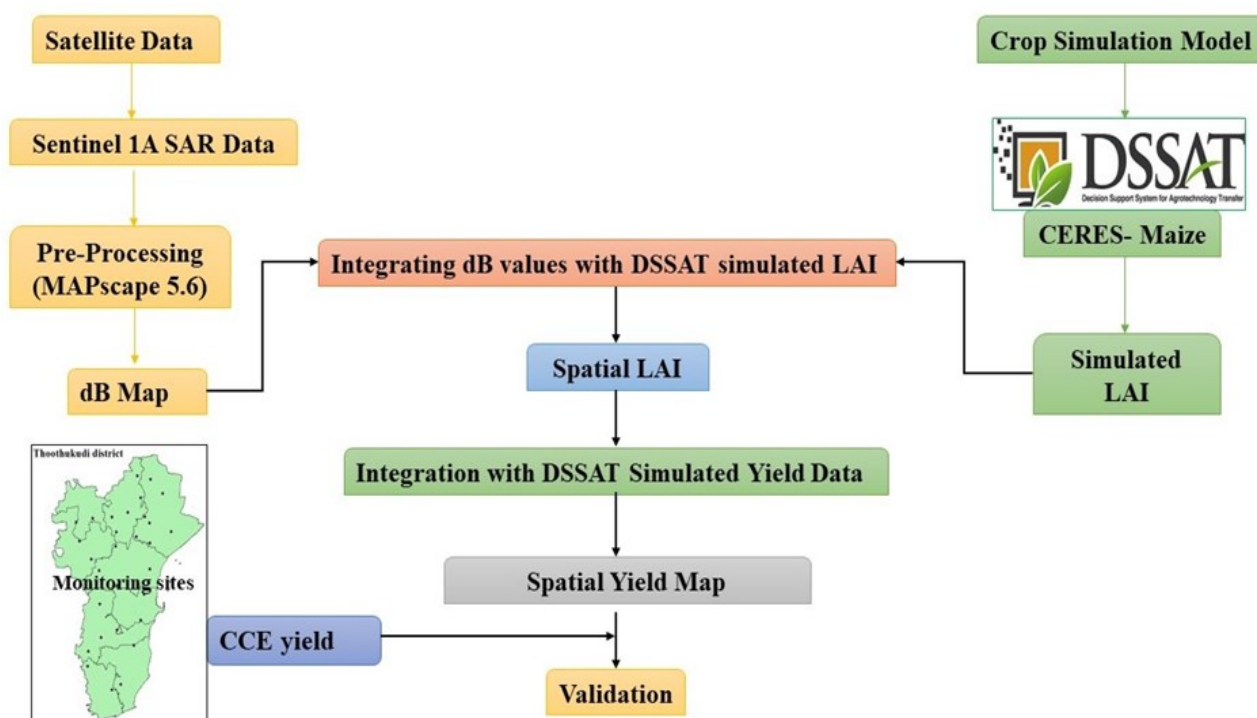


Fig. 4. Schematic representation of the Maize yield estimation by integrating SAR satellite products and the DSSAT CERES-Maize model

yield

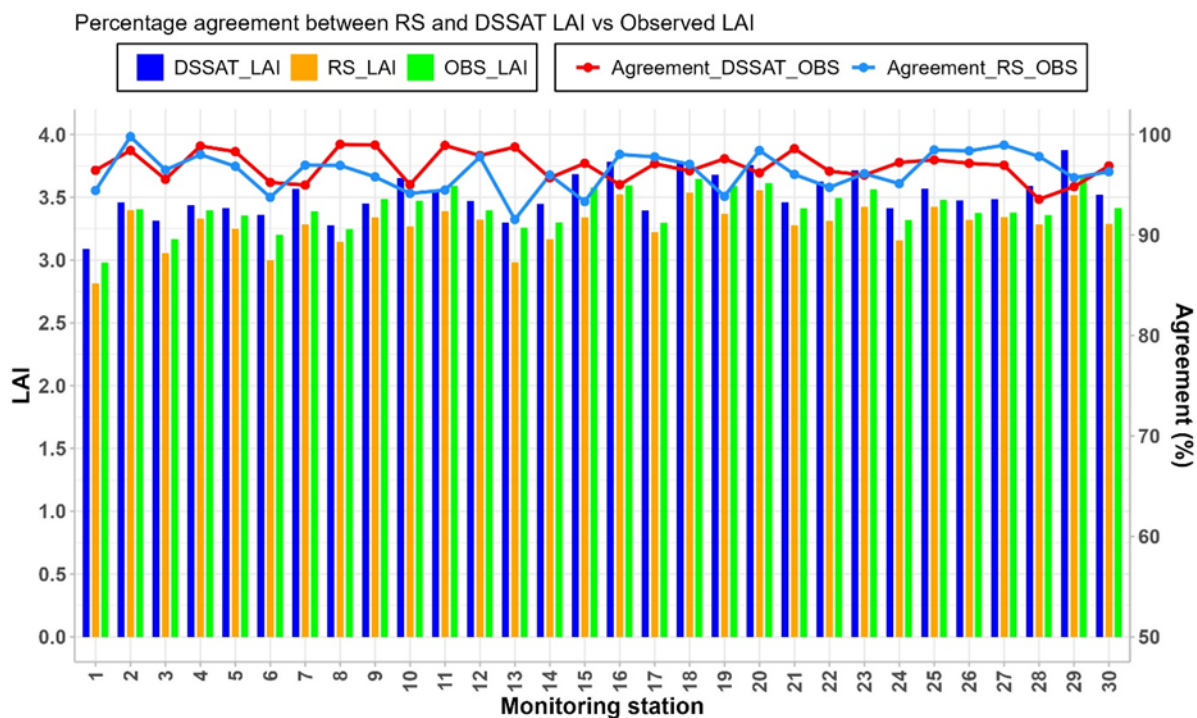


Fig. 5. DSSAT simulated LAI, Remote Sensing (RS) LAI, Observed LAI and concordance between them

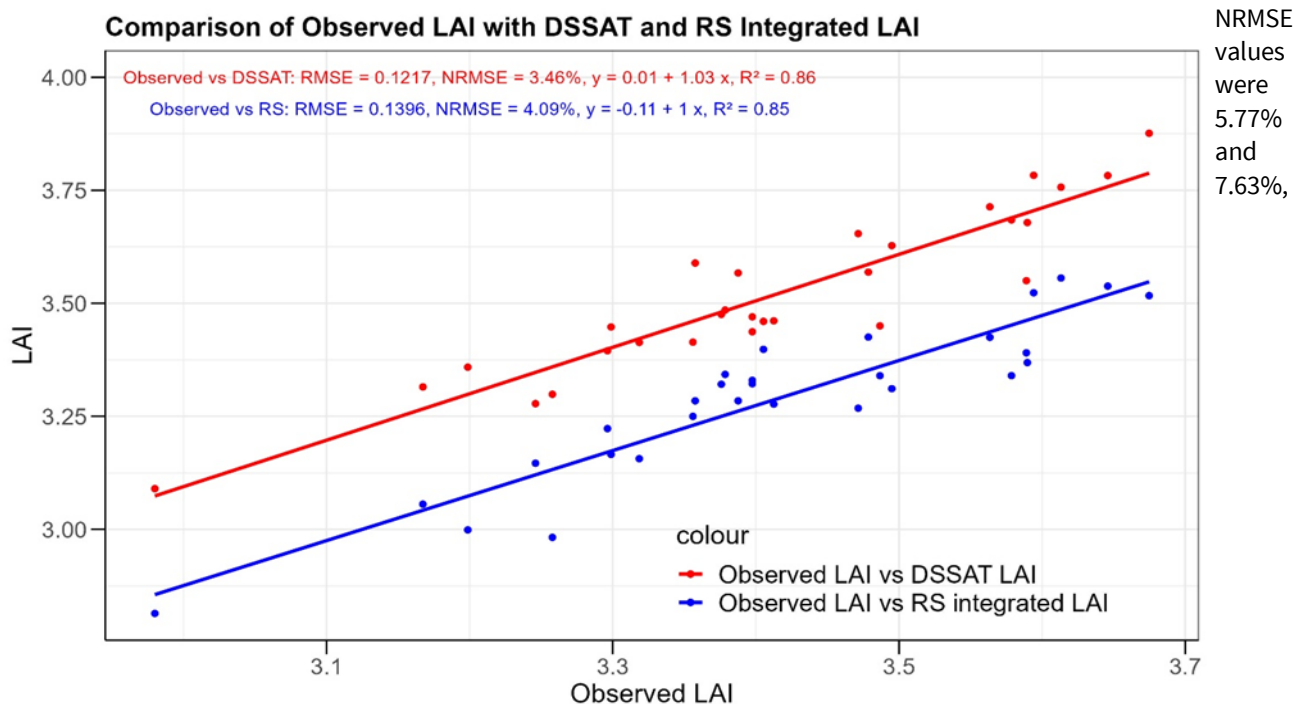


Fig. 6. Correlation between observed and modelled LAI

averaged 7533.9 kg/ha, and CCE yield averaged 8096.6 kg/ha (Fig. 9). The DSSAT model recorded the highest yield at 9723 kg/ha, while the RS method reported the lowest yield at 6035 kg/ha.

The concordance between DSSAT and CCE yield values ranged from 88.75% to 99.64%, demonstrating a high consistency overall. Similarly, the concordance between RS and CCE yield values varied between 86.09% and 98.48%. Statistical analysis revealed that the coefficient of determination was 0.854 for the DSSAT-CCE comparison and 0.867 for the RS-CCE comparison, indicating linear solid relationships in both cases. The RMSE was calculated to be 466.84 kg/ha for DSSAT and 617.94 kg/ha for RS, while the

respectively, indicating that DSSAT provided predictions closer to the observed CCE yield values. The spatial yield distribution is depicted in Fig.10.

Discussion

Leaf Area Index Estimation

The results highlight fundamental differences between the RS and DSSAT models in estimating LAI. While effective in capturing LAI variability, the RS model shows some limitations in accuracy, as evidenced by its higher RMSE and NRMSE values. These limitations could be attributed to factors such as the spatial resolution of remote sensing data and potential errors in satellite imagery interpretation. Despite these challenges, the RS model provides a valuable

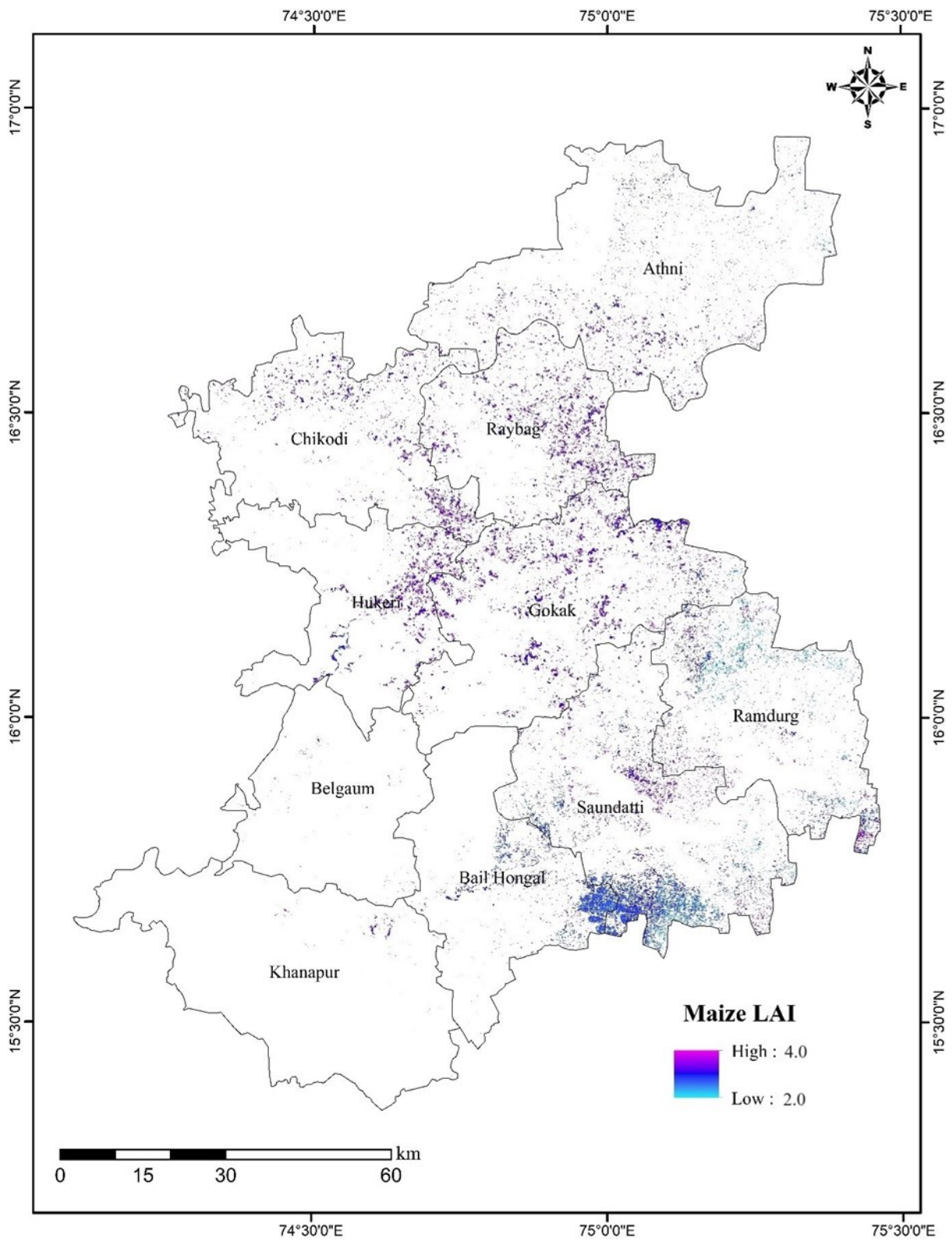


Fig. 7. Spatial LAI map of Belagavi district

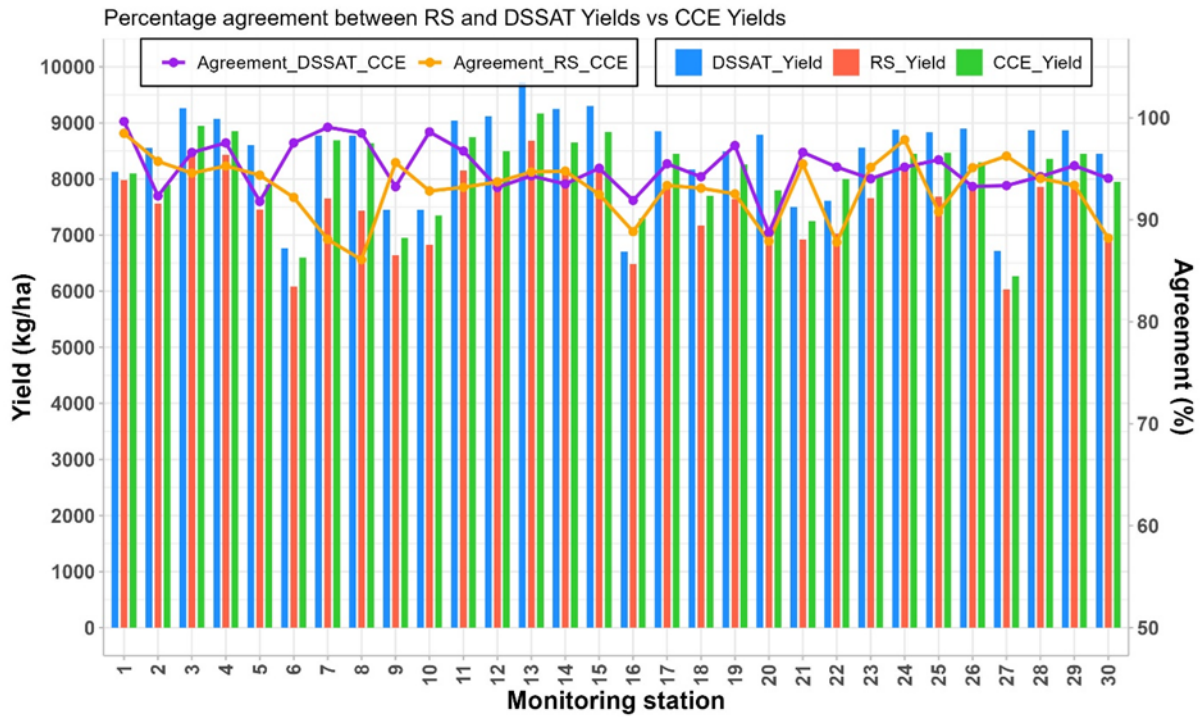


Fig. 8. DSSAT simulated yield, Remote Sensing (RS) yield, CCE yield and concordance between them

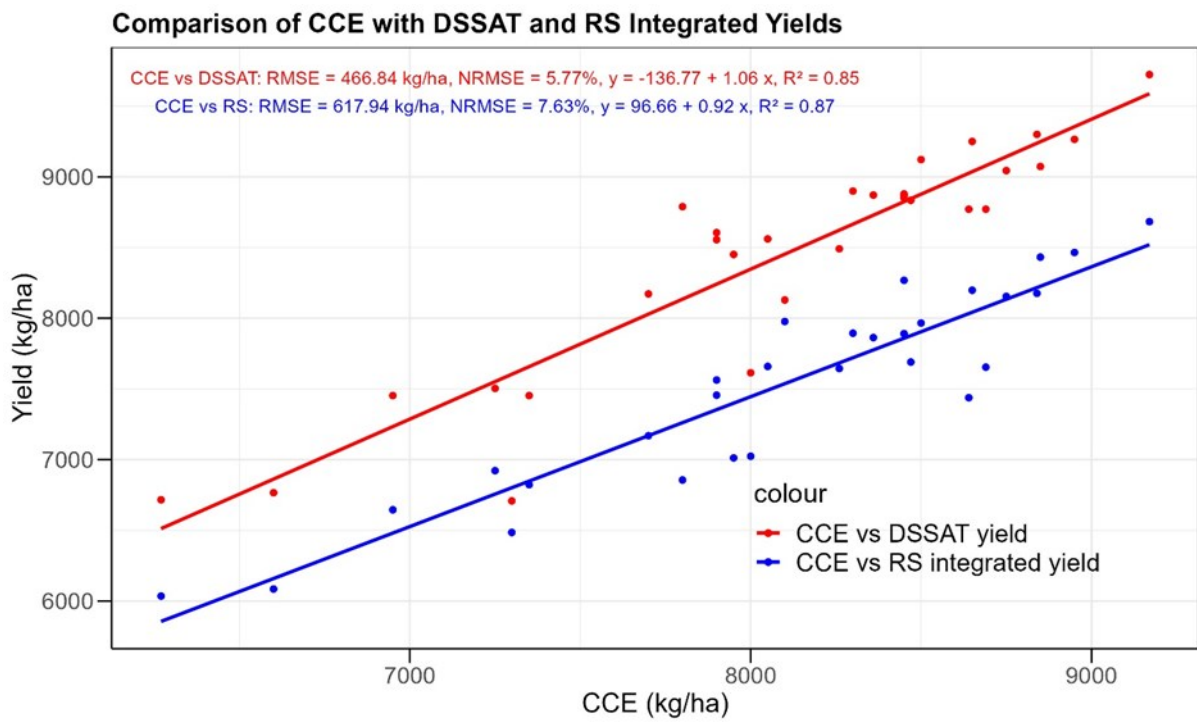


Fig. 9. Correlation between modelled and CCE yield

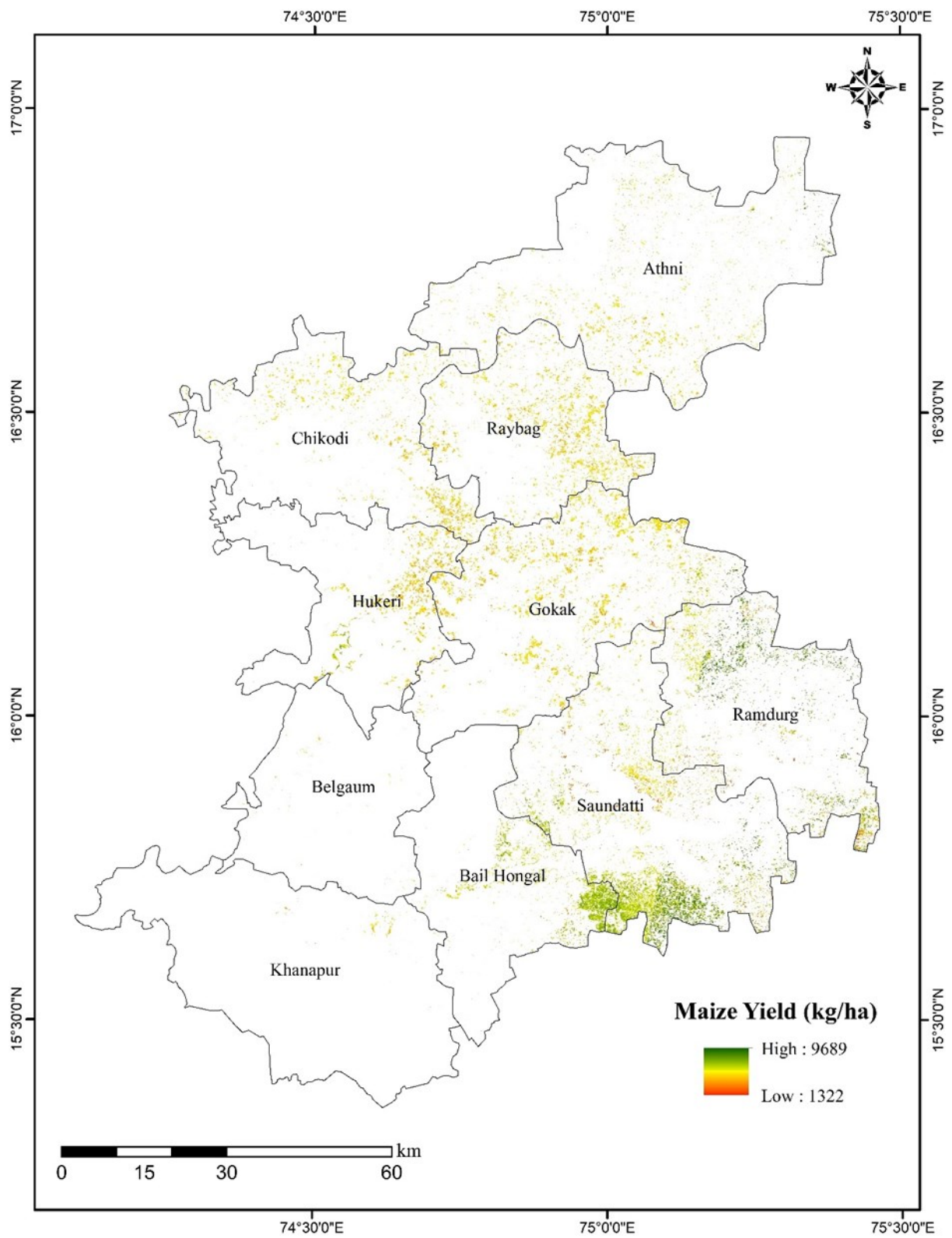


Fig. 10. Spatial yield map of Belagavi district

tool for large-scale agricultural monitoring, especially in regions where ground-based data collection is challenging (18).

The DSSAT model, with its more detailed simulation of crop growth dynamics and incorporation of site-specific factors, demonstrates superior accuracy in LAI estimation. Its higher R^2 value and lower error metrics suggest it is more reliable for precise LAI predictions. This makes the DSSAT model particularly useful for site-specific agricultural applications requiring detailed crop management decisions (19).

The findings suggest that while the DSSAT model generally offers better accuracy (94 %), the RS model's (92 %) ability to cover large areas quickly and efficiently should not be overlooked. Integrating both models could potentially enhance overall LAI estimation, combining the spatial coverage of RS with the detailed crop growth simulation of DSSAT. This approach could provide more robust tools for precision agriculture and improve resource management and crop productivity (20).

Maize Yield Estimation

The results suggest that the DSSAT model offers yield predictions closely aligned with observed CCE data. The high agreement percentages and the lower RMSE and NRMSE values indicate that DSSAT is a reliable tool for yield estimation, likely due to its detailed modelling of crop growth processes (21; 22). The strong correlation between DSSAT and CCE yields is consistent with other studies that have validated DSSAT's accuracy in different agricultural settings (2).

In contrast, while RS data also showed a strong correlation with CCE yield, the higher RMSE and NRMSE values suggest more significant variability and potential inaccuracies in yield estimation using this method. This variability may be attributed to limitations in remote sensing techniques, such as spatial resolution constraints or environmental factors that may not be fully captured in RS data (23; 5).

The R^2 values for DSSAT and RS compared to CCE indicate that both methods can explain a significant portion of the variability in observed yields, with RS showing a slightly stronger correlation. However, the lower prediction errors associated with DSSAT suggest that it is more precise in yield estimation. This precision is crucial for making informed agricultural decisions and improving crop management practices.

These findings underscore the complementary strengths of DSSAT and RS methods in yield prediction. DSSAT's process-based modelling approach allows for more precise yield predictions, while RS offers valuable large-scale yield estimates that can be integrated with ground-based observations. Combining these methods could enhance the accuracy and scalability of yield predictions, providing a more robust tool for agricultural planning and decision-making (24).

Conclusion

The study successfully integrated Sentinel-1A SAR data with the DSSAT CERES-Maize crop simulation model to estimate LAI and maize yield. Ground truth data collection and CCE were used to validate the accuracy of these methods. The analysis of LAI revealed strong correlations between Remote Sensing RS, DSSAT model outputs and observed data. While RS data showed higher agreement with observed LAI, the DSSAT model had slightly lower RMSE and NRMSE values, indicating a closer fit to ground-truth measurements. The DSSAT model demonstrated high accuracy for maize yield estimation, with linear solid relationships and lower prediction errors than RS data, which showed more significant variability. This study highlights the complementary strengths of RS and DSSAT methods in crop monitoring and yield prediction, emphasizing their potential for improving agricultural assessments and informed decision-making in diverse landscapes.

Acknowledgements

This work is part of the "MNCFC - Pilot Studies for GP level crop estimation using advanced technologies for non-cereal crops" project.

Authors' contributions

Conceptualization: HT and PS; Data curation: SNS and SS.; Formal analysis: HT, PS, SNS, RKP and SNK; Funding acquisition: PS and RKP; Investigation: SNK, RKP and SAP; Methodology: HT, PS and SNS; Project administration: PS, RKP and SAP; Resources: RKP, SS and VS; Software: SNS, RKP, PK and SS.; Supervision: PS, RKP, SNK, VS and APS; Validation: HT and SNS; Visualization: SNS and SS; Writing-original draft: HT and PS; Writing-review & editing, SNS, SNK, SAP, PK and VS. All authors have read and agreed to the published version of the manuscript.

Compliance with ethical standards

Conflict of interest: Authors do not have any conflict of interest to declare.

Ethical issues: None.

References

1. Agriculture and Food, World Bank. 2022. <https://www.worldbank.org/en/topic/agriculture/overview>
2. World Employment and Social Outlook: Trends 2024, International Labour Organisation. <https://www.ilo.org/publications/flagship-reports/world-employment-and-social-outlook-trends-2024>
3. Population Reference Bureau, World population data sheet. 2023. <https://2023-wpds.prb.org/>
4. Lobell DB, Asseng S. Comparing estimates of climate change impacts from process-based and statistical crop models. *Environ Res Lett.* 2017;12(1):015001. <https://iopscience.iop.org/article/10.1088/1748-9326/aa518a>
5. Ahmad I, Saeed U, Fahad M, Ullah A, Rahman MH, Ahmad A, Judge J. Yield forecasting of spring maize using remote sensing

- and crop modeling in Faisalabad-Punjab Pakistan. *J Indian Soc Remote Sens.* 2018;46:1701-1711. <https://doi.org/10.1007/s12524-018-0825-8>
6. Fermont AM, Benson T. Estimating yield of food crops grown by smallholder farmers. *Int. Food Policy Res. Inst.* 2011; Working Paper 27. https://www.researchgate.net/publication/254416399_Estimating_yield_of_food_crops_grown_by_smallholder_farmers_A_review_in_the_Uganda_context
 7. Setiyono TD, Quicho ED, Holecz FH, Khan NI, Romuga G, Maunahan A, Garcia C, et al. Rice yield estimation using synthetic aperture radar (SAR) and the ORYZA crop growth model: development and application of the system in South and South-east Asian countries. *Int J Remote Sens.* 2019;40(21):8093-8124. <https://doi.org/10.1080/01431161.2018.1547457>
 8. Huang J, Gómez-Dans JL, Huang H, Ma H, Wu Q, Lewis PE, Liang S, et al. Assimilation of remote sensing into crop growth models: Current status and perspectives. *Agric For Meteorol.* 2019;276:107609. <https://doi.org/10.1016/j.agrformet.2019.06.008>
 9. Jones JW, Hoogenboom G, Porter CH, Boote KJ, Batchelor WD, Hunt LA, et al. The DSSAT cropping system model. *Eur J Agron.* 2003;18(3-4):235-265. [https://doi.org/10.1016/S1161-0301\(02\)00107-7](https://doi.org/10.1016/S1161-0301(02)00107-7)
 10. Corbeels M, Chirat G, Messad S, Thierfelder C. Performance and sensitivity of the DSSAT crop growth model in simulating maize yield under conservation agriculture. *Eur. J. Agron.* 2016;76:41-53. <https://doi.org/10.1016/j.eja.2016.02.001>
 11. Dorigo W, Zurita-Milla R, de Wit A, Brazile J, Singh R, Schaepman ME. A review on reflective remote sensing and data assimilation techniques for enhanced agricultural monitoring. *Int J Appl Earth Obs. Geoinf.* 2015;18:191-204. <https://doi.org/10.1016/j.jag.2006.05.003>
 12. Basso B, Cammarano D, Carfagna E. Review of crop yield forecasting methods and early warning systems. In: *First Meeting of the Scientific Advisory Committee of the Global Strategy to Improve Agricultural and Rural Statistics.* 2013. https://www.fao.org/fileadmin/templates/ess/documents/meetings_and_workshops/GS_SAC_2013/Improving_methods_for_crops_estimates/Crop_Yield_Forecasting_Methods_and_Early_Warning_Systems_Lit_review.pdf
 13. Directorate of Economics and Statistics, Ministry of Agriculture and Farmers Welfare, Govt. of India Accessed on August 01, 2024. <https://data.desagri.gov.in/website/crops-apy-report-web>
 14. Ramachandra TV, Setturu B. Ecologically sensitive regions in Belgaum district, Karnataka, Central Western Ghats. *J Environ Biol.* 2023;44(1):11-26. <https://doi.org/10.22438/jeb/44/1/MRN-5041>
 15. Amrutha Rani HR, Shreedhar R. Study of rainfall trends and variability for Belgaum. *Int J Res Eng Technol.* 2014;3(6):148-155.
 16. Carlotto MJ. Effect of errors in ground truth on classification accuracy. *Int J Remote Sens.* 2009;30(18):4831-4849. <https://doi.org/10.1080/01431160802672864>
 17. Ali U, Esau TJ, Farooque AA, Zaman QU, Abbas F, Bilodeau MF. Limiting the collection of ground truth data for land use and land cover maps with machine learning algorithms. *ISPRS Int J Geo-Inf.* 2022;11(6):333. <https://doi.org/10.3390/ijgi11060333>
 18. Dasari K, Anjaneyulu L, Nadimikeri J. Application of C-band sentinel-1A SAR data as proxies for detecting oil spills of Chennai, East Coast of India. *Mar Pollut Bull.* 2022;174:113182. <https://doi.org/10.1016/j.marpolbul.2021.113182>
 19. Alaska Satellite Facility DAAC (ASF DAAC). Accessed on April 15, 2024. <https://asf.alaska.edu/>
 20. Castriotta AG, Volpi F. Copernicus sentinel data access annual report 2022. *Annu. Rep.* 2022. <https://sentiwiki.copernicus.eu/web/document-library>
 21. Wu B, Zhang M, Zeng HW, Tian FY, Potgieter AB, Qin X, Yan N, et al. Challenges and opportunities in remote sensing-based crop monitoring: A review. *Nat Sci Rev.* 2023;10(4). <https://doi.org/10.1093/nsr/nwac290>
 22. Corbeels M, Chirat G, Messad S, Thierfelder C. Performance and sensitivity of the DSSAT crop growth model in simulating maize yield under conservation agriculture. *Eur J Agron.* 2016;76:41-53. <https://doi.org/10.1016/j.eja.2016.02.001>
 23. Gumma MK, Nukala RM, Panjala P, Bellam PK, Gajjala S, Dubey SK, Sehgal VK, Mohammed I, Deevi KC. Optimizing crop yield estimation through geospatial technology: A comparative analysis of a semi-physical model, crop simulation, and machine learning algorithms. *AgriEngineering.* 2024;6(1):786-802. <https://doi.org/10.3390/agriengineering6010045>
 24. Pazhanivelan S, Geethalakshmi V, Tamilmounika R, Sudarmanian NS, Kaliaperumal R, Ramalingam K, Sivamurugan AP, Mrunalini K, Yadav MK, Quicho ED. Spatial rice yield estimation using multiple linear regression analysis, semi-physical approach and assimilating SAR satellite-derived products with DSSAT crop simulation model. *Agronomy.* 2022;12(9):2008. <https://doi.org/10.3390/agronomy12092008>
 25. Hoogenboom G, Porter CH, Boote KJ, Shelia V, Wilkens PW. *Decision Support System for Agrotechnology Transfer (DSSAT) Version 4.7.* Gainesville: DSSAT Foundation. 2019. https://link.springer.com/chapter/10.1007/978-94-017-3624-4_8
 26. Dong J, Xiao X, Menarguez MA, Zhang G, Qin Y, Luo P, Zhang Y. Mapping paddy rice planting area in northeastern Asia with Landsat 8 images, phenology-based algorithm and Google Earth Engine. *Remote Sens. Environ.* 2016;185:142-154. <https://doi.org/10.1016/j.rse.2016.02.016>
 27. Cui Y, Liu S, Li X, Geng H, Xie Y, He Y. Estimating maize yield in the black soil region of Northeast China using land surface data assimilation: integrating a crop model and remote sensing. *Front Plant Sci.* 2022;13:915109. <https://doi.org/10.3389/fpls.2022.915109>
 28. NASA Power. Accessed on June 21, 2024. <https://power.larc.nasa.gov/>
 29. Harvard Dataverse. Accessed on June 22, 2024. <https://doi.org/10.7910/DVN/1PEEY0>